

Supporting Information

Self-Reporting Photoluminescent Porous Silicon Microparticles for Drug Delivery

Joanna Wang¹, Tushar Kumeria^{2,3}, Maria Teresa Bezem⁴, Jian Wang⁵, Michael J. Sailor^{2}*

¹Material Science and Engineering Program, University of California, San Diego, 9500 Gilman Drive, La Jolla, CA 92093-0358, USA;

²Department of Chemistry and Biochemistry, University of California, San Diego, 9500 Gilman Drive, La Jolla, CA 92093-0358, USA;

³School of Pharmacy, The University of Queensland, 20 Cornwall Street, Woolloongabba, Queensland 4102, Australia

⁴Department of Biomedicine, University of Bergen, Jonas Lies vei 91, N-5020 Bergen, Norway

⁵School of Physics and Electronic Information Engineering, Henan Polytechnic University, Jiaozuo 454000, China

*Corresponding author. Michael J. Sailor email address: msailor@ucsd.edu

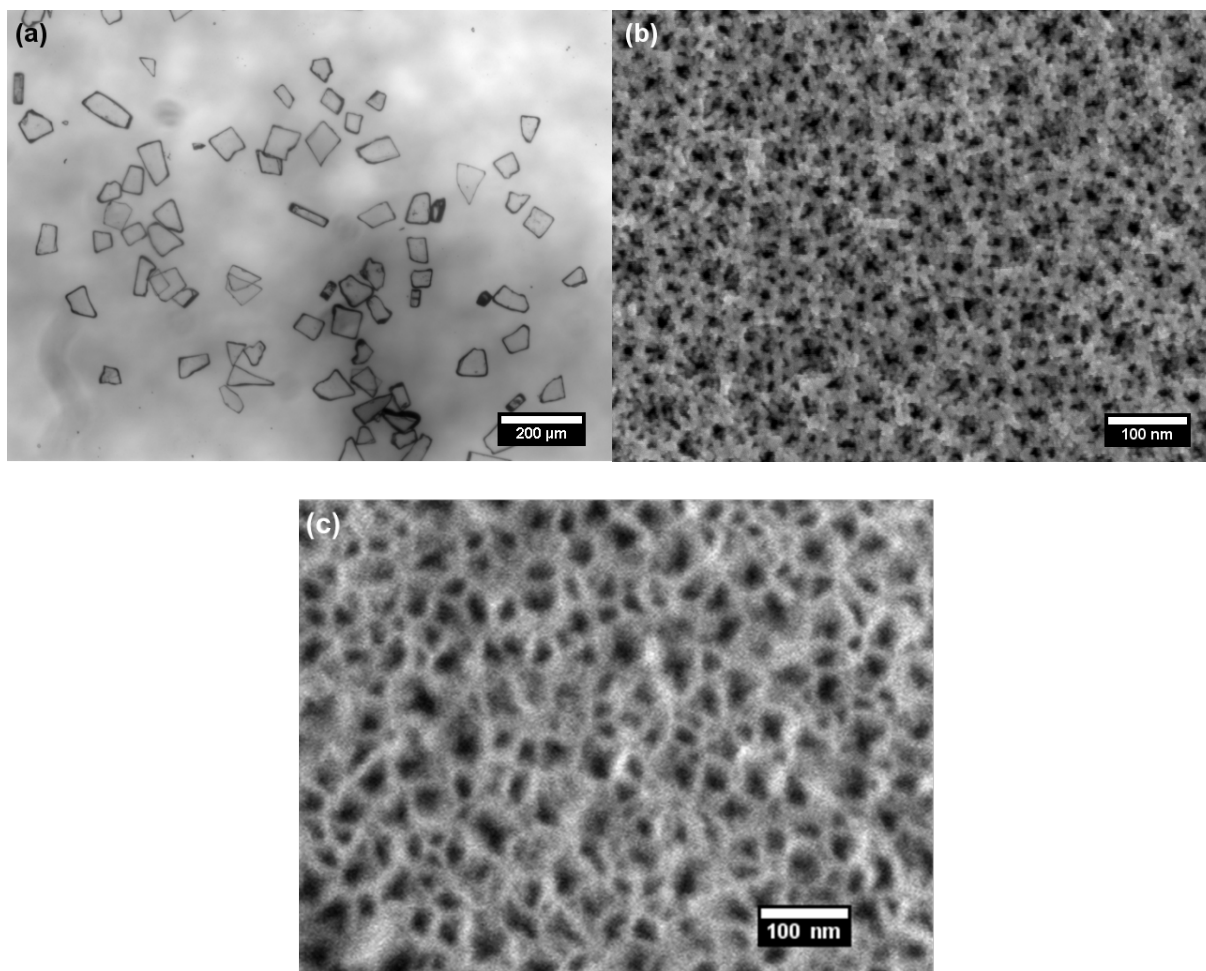


Figure S1. Representative (a) bright field optical microscope images of oxidized (700°C for 45 min) pSi particles (5X); (b) Plan-view SEM (secondary electron) image of the pores in a "small-pore" sample (see Table 1), obtained from the pSi film etched into a silicon wafer prior to microparticle formation and subsequent oxidation, and (c) plan-view SEM (secondary electron) image of the pores in a "large-pore" sample, obtained from the pSi film etched into a silicon wafer prior to microparticle formation and subsequent oxidation (see Table 2).

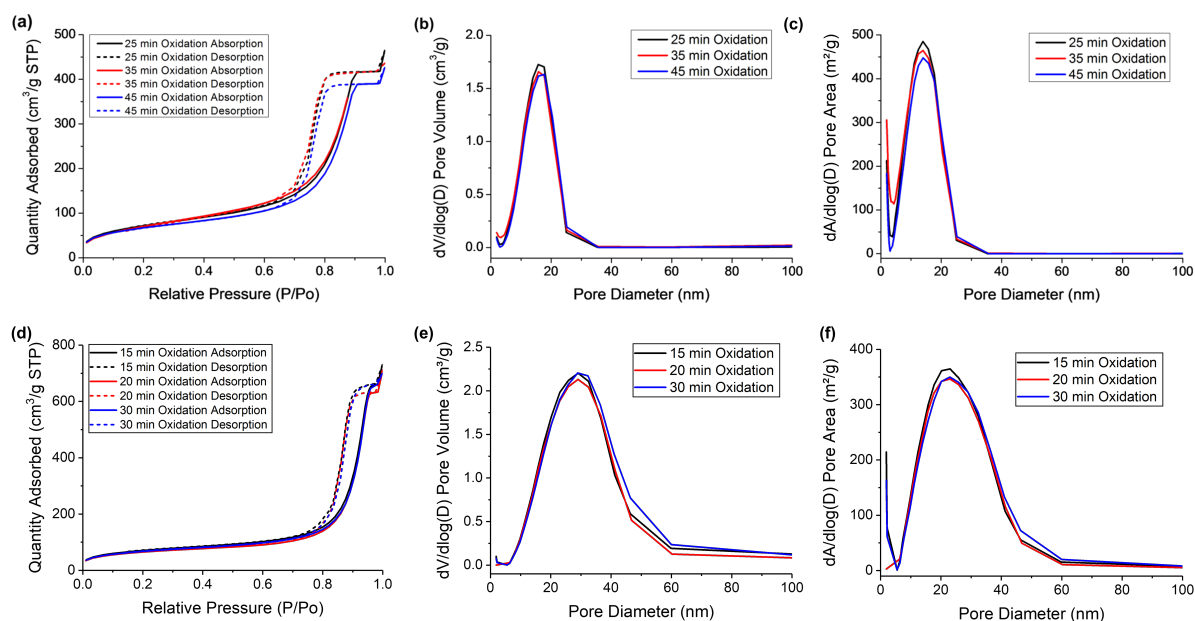


Figure S2. Characterization of porous silicon particles by nitrogen adsorption/desorption isotherms. These particles were characterized prior to thermal oxidation, and represent the two types of etching conditions used in this study: "small-pore" (a-c) and "large-pore" (d-f). Adsorption-desorption isotherms shown in (a) and (d); Calculated BJH pore volume with respect to pore diameter shown in (b) and (e); pore area with respect to pore diameter shown in (c) and (f). The "small-pore" samples of (a), (b), and (c) were prepared by etching the Si wafers at a constant current density of 70 mA/cm^2 for 600 s in 3:1 (v:v) 48% aqueous HF: absolute ethanol and their properties are summarized in Table 1 of the main text. The "large-pore" samples of (d), (e), and (f) were prepared by etching the Si wafers at a constant current density of 30 mA/cm^2 for 720 s in 1:1 (v:v) 48% aqueous HF: absolute ethanol and their properties are summarized in Table 2 of the main text.

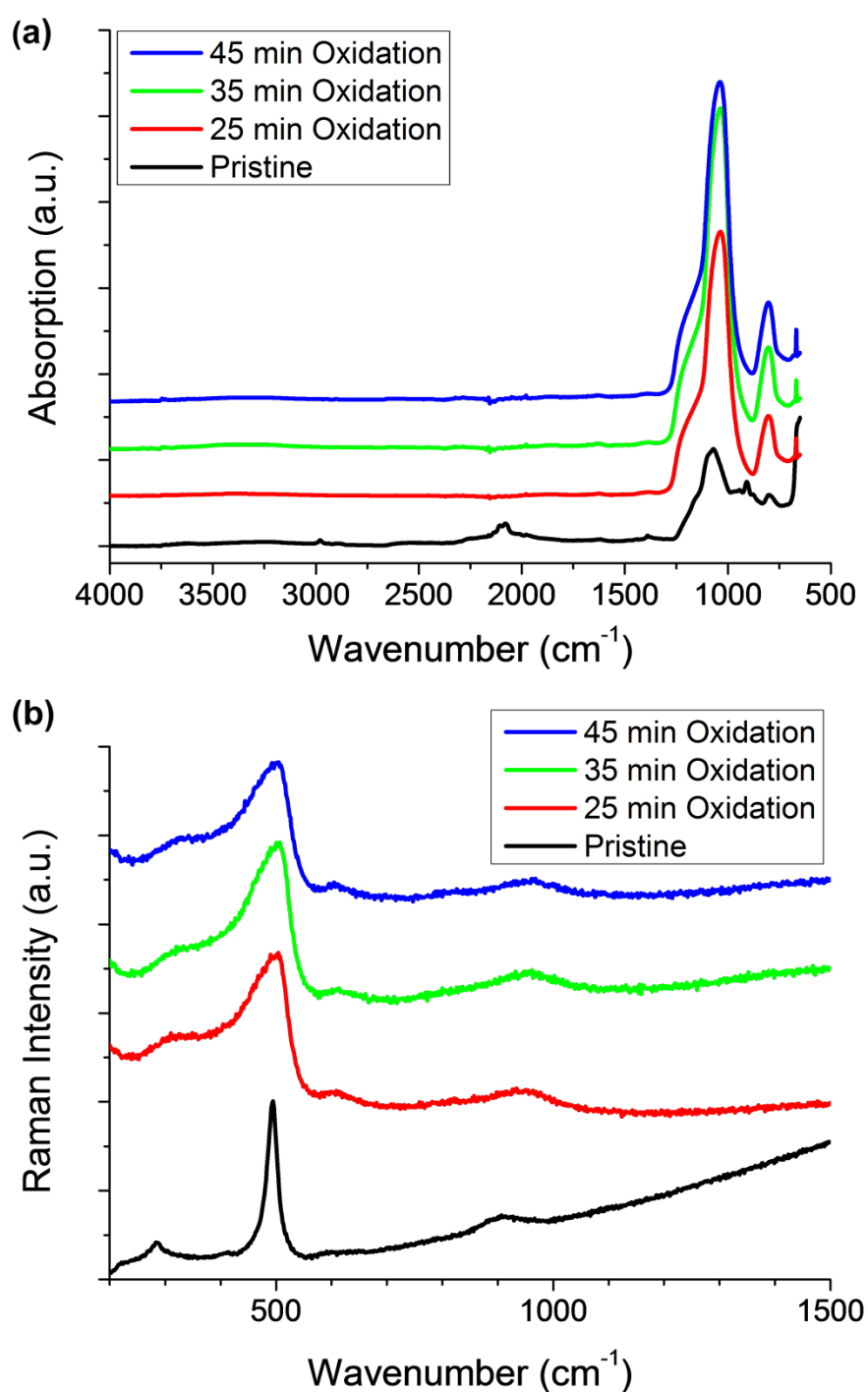


Figure S3. Characterization of porous silicon particles before ("Pristine") and after thermal oxidation at 700°C for the indicated times. These samples were all "small-pore" microparticles, prepared to contain ~10 nm pores (Table 1). (a) Attenuated total reflectance Fourier-transform infrared (ATR-FTIR) spectra reveal the removal of surface Si-H groups and conversion to Si-O-Si after oxidation. (b) Raman spectra obtained after oxidation shows the Si lattice mode associated with the crystalline silicon skeleton.

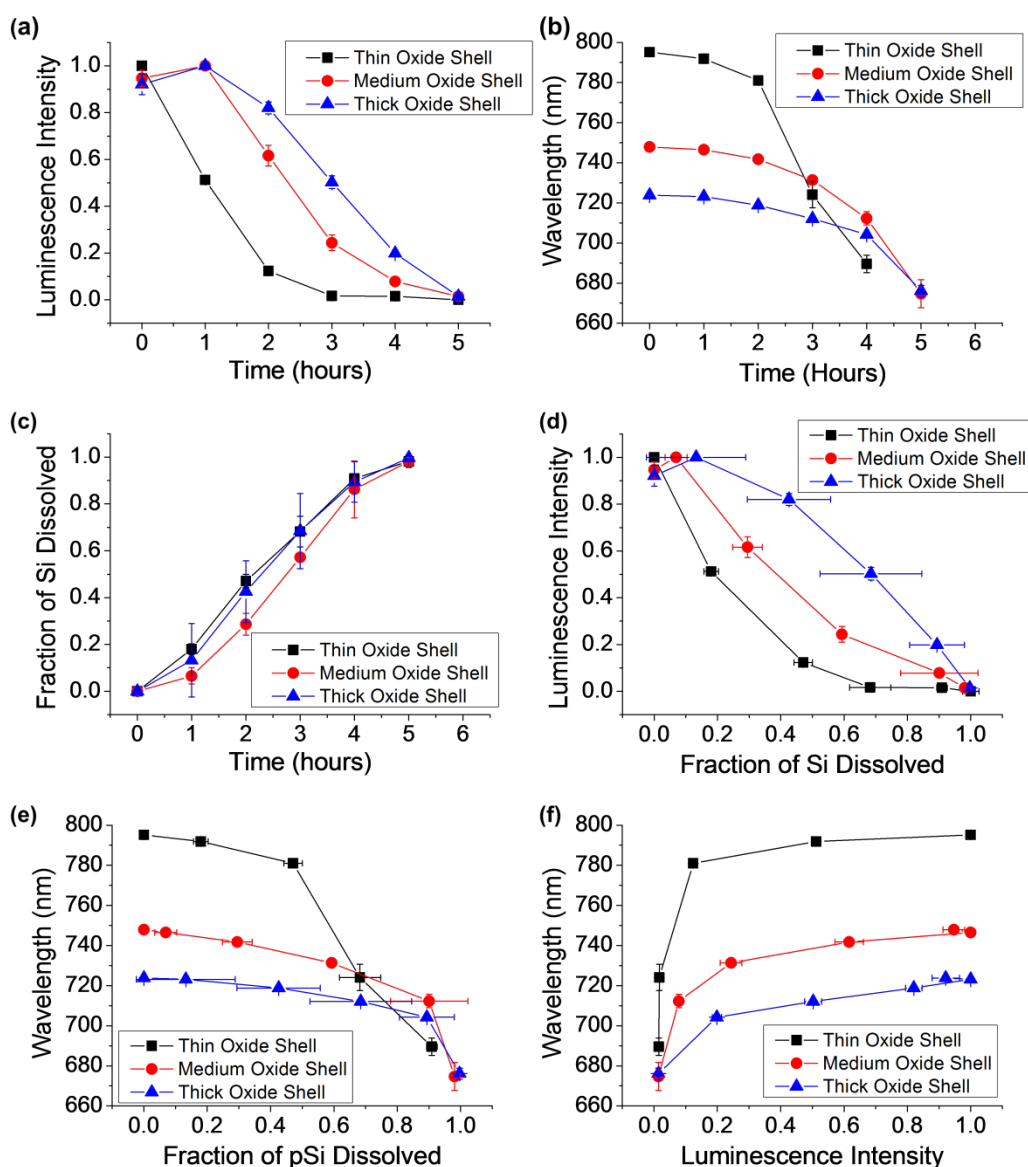


Figure S4. Correlations of photoluminescence intensity, photoluminescence wavelength, and fraction of Si dissolved with time exposed to the accelerated dissolution conditions (0.1 M KOH) for three different formulations of core-shell porous Si-SiO₂ particles, loaded with bovine serum albumin (BSA) by the electrostatic adsorption method. The three formulations were prepared with different SiO₂ shell thickness and core size by thermal oxidation at 700 °C for the indicated times. Traces designated "25 min oxidation", "35 min oxidation", and "45 min oxidation" correspond to the "thin oxide shell", "medium oxide shell", and "thick oxide shell" samples, respectively, as discussed in the text. Oxide thickness increased and core diameter decreased with increasing oxidation time. These samples were all "small-pore" microparticles, prepared to contain ~10 nm pores (Table 1). (a) Normalized photoluminescence intensity ($\lambda_{\text{ex}} = 365 \text{ nm}$) as a function of time. (b) Wavelength of maximum photoluminescence ($\lambda_{\text{ex}} = 365 \text{ nm}$) as a function of time. (c) Fraction of silicon matrix dissolved as a function of time. Mass of dissolved Si was quantified by Molybdenum Blue assay. (d) Normalized photoluminescence intensity as a function of fraction of silicon dissolved. (e) Wavelength of maximum photoluminescence ($\lambda_{\text{ex}} = 365 \text{ nm}$) as a function of fraction of silicon dissolved. (f) Wavelength of maximum photoluminescence ($\lambda_{\text{ex}} = 365 \text{ nm}$) as a function of normalized photoluminescence intensity. Error bars represent standard deviation (n=3).

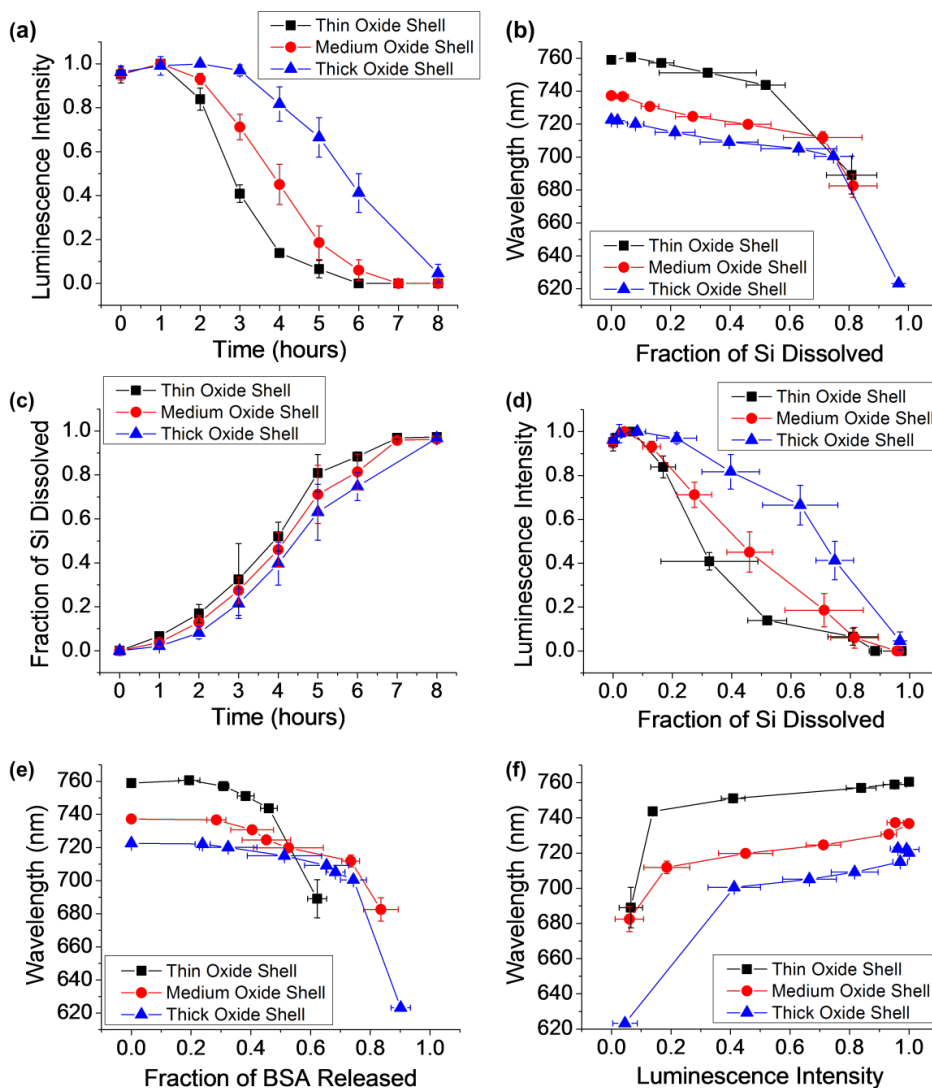


Figure S5. Correlations of photoluminescence intensity, photoluminescence wavelength, and fraction of Si dissolved with time exposed to the accelerated dissolution conditions (0.1 M KOH) for three different formulations of core-shell porous Si-SiO₂ particles, loaded with bovine serum albumin (BSA) by the magnesium silicate trapping method. The three formulations were prepared with different SiO₂ shell thickness and core size by thermal oxidation at 700 °C for the indicated times. Traces designated "25 min oxidation", "35 min oxidation", and "45 min oxidation" correspond to the "thin oxide shell", "medium oxide shell", and "thick oxide shell" samples, respectively, as discussed in the text. These samples were all "small-pore" microparticles, prepared to contain ~10 nm pores (Table 1). BSA was trapped in the porous Si-SiO₂ particles by means of precipitation of magnesium silicate concomitant with BSA loading as described in Figure 2. (a) Normalized photoluminescence intensity ($\lambda_{ex} = 365$ nm) as a function of time. (b) Wavelength of maximum photoluminescence ($\lambda_{ex} = 365$ nm) as a function of time. (c) Fraction of silicon matrix dissolved as a function of time. Mass of dissolved Si was quantified by Molybdenum Blue assay. (d) Normalized photoluminescence intensity as a function of fraction of silicon dissolved. (e) Wavelength of maximum photoluminescence ($\lambda_{ex} = 365$ nm) as a function of fraction of silicon dissolved. (f) Wavelength of maximum photoluminescence ($\lambda_{ex} = 365$ nm) as a function of normalized photoluminescence intensity. Error bars represent standard deviation (n=3).

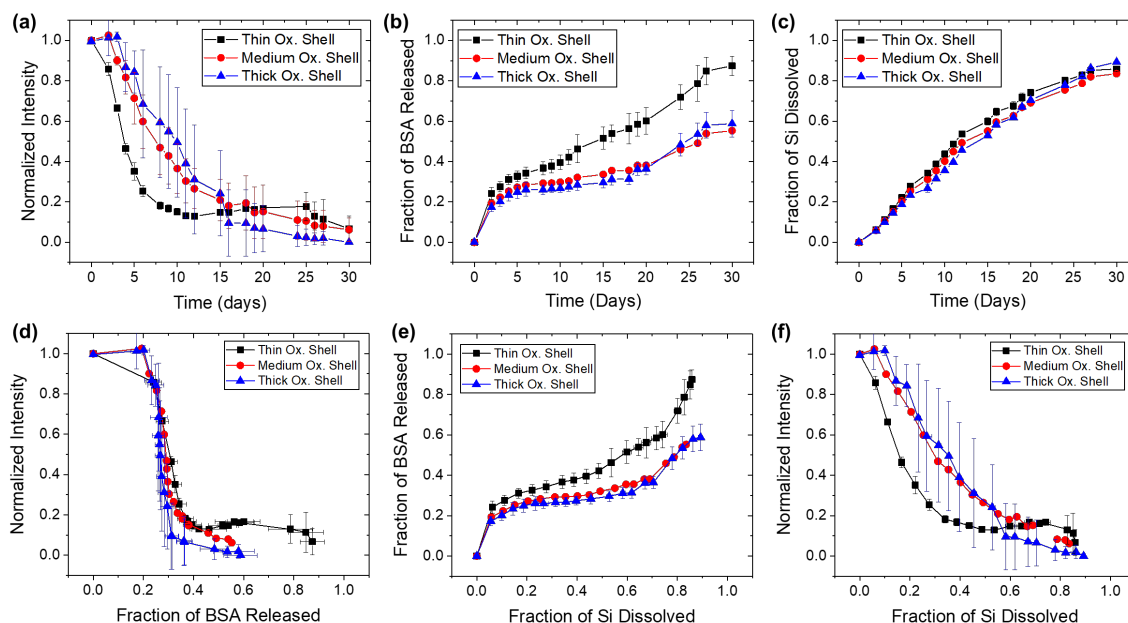


Figure S6. Correlations between photoluminescence from the Si skeletal core, protein released, silicon dissolved, and time for adsorption-loaded core-shell porous Si-SiO₂ particles as they undergo dissolution in aqueous PBS (pH = 7.4) at 37 °C. Traces designated "Thin Ox. Shell", "Medium Ox. Shell", and "Thick Ox. Shell" correspond to pSi particles where the skeletal core was oxidized at 700 °C for 15 min, 20 min, and 30 min, respectively, prior to protein loading. These samples were all "large-pore" microparticles, prepared to contain ~20 nm pores (Table 2) (a) Integrated photoluminescence intensity (in wavelength range 600 - 800 nm) from particles as a function of time. (b) Fraction of bovine serum albumin (BSA) released from the particles as a function of time. (c) Fraction of silicon dissolved as a function of time. (d) Integrated photoluminescence intensity from particles as a function of fraction of BSA released. (e) Fraction of BSA released as a function of silicon dissolved. (f) Integrated luminescence intensity as a function of silicon dissolved. Error bars represent standard deviation (n = 2 for the medium oxide shell samples; n = 3 for all other samples).